Electronic structures of interfacial states formed at polymeric semiconductor heterojunctions

YA-SHIH HUANG[1,2], SEBASTIAN WESTENHOFF[1]*, IGOR AVILOV[2], PAIBOON SREEARUNOTHAI[1†], JUSTIN M. HODGKISS[1], CAROLINE DELEENER[2], RICHARD H. FRIEND[1‡] AND DAVID BELJONNE[2‡]

[1]Cavendish Laboratory, University of Cambridge, J J Thomson Avenue, Cambridge, CB3 0HE, UK
[2]Laboratory for Chemistry of Novel Materials, University of Mons-Hainaut, Place du Parc 20, B-7000 Mons, Belgium
*Present address: Department of Chemistry, Biochemistry and Biophysics, Gothenburg University, 40530 Gothenburg, Sweden
†Present address: Chemistry Department, Building 555A, Brookhaven National Lab, Upton, New York 11973-5000, USA
‡e-mail: rhf10@cam.ac.uk; David@averell.umh.ac.be

Published online: 27 April 2008; doi:10.1038/nmat2182

Heterojunctions between organic semiconductors are central to the operation of light-emitting and photovoltaic diodes, providing respectively for electron–hole capture and separation. However, relatively little is known about the character of electronic excitations stable at the heterojunction. We have developed molecular models to study such interfacial excited electronic excitations that form at the heterojunction between model polymer donor and polymer acceptor systems: poly(9,9-dioctylfluorene-co-bis-*N*,*N*-(4-butylphenyl)-bis-*N*,*N*-phenyl-1,4-phenylenediamine) (PFB) with poly(9,9-dioctylfluorene-co-benzothiadiazole) (F8BT), and poly(9,9-dioctylfluorene-co-*N*-(4-butylphenyl)diphenylamine) (TFB) with F8BT. We find that for stable ground-state geometries the excited state has a strong charge-transfer character. Furthermore, when partly covalent, modelled radiative lifetimes ($\sim 10^{-7}$ s) and off-chain axis polarization (30°) match observed 'exciplex' emission. Additionally for the PFB:F8BT blend, geometries with fully ionic character are also found, thus accounting for the low electroluminescence efficiency of this system.

The so-called 'type-II' heterojunctions[1] are usually used in organic optoelectronic devices so that both the highest-occupied-molecular-orbital (HOMO) and the lowest-unoccupied-molecular-orbital (LUMO) levels of one polymer lie higher in energy than the corresponding levels in the other polymer. Depending on the energy mismatch between the frontier orbitals, type-II heterojunctions can either facilitate charge separation in photovoltaic cells[2–4] or enhance quantum yields in light-emitting diodes[1,5–7]. For the case of photovoltaic diodes, there is considerable evidence in the literature for very rapid photoinduced electron transfer as the photogenerated exciton reaches the heterojunction. This is generally inferred from the rapid appearance of excited-state optical absorption characteristic of polaron-like charged states. However, there is evidence that the electron and hole remain bound as a charge-transfer exciton—for example that recombination is predominantly geminate[8]. For some materials systems, including those studied (see Fig. 1a for chemical structures), the charge-transfer exciton shows sufficient overlap of electron and hole wavefunctions that there is significant luminescence (characterized by a much-increased radiative lifetime, to about 100 ns, and a substantial red-shift); these have been termed 'exciplexes'. A detailed picture has been built up for these systems[1,9–17], which we match here to quantum-chemical modelling of these charge-transfer excitations.

The formation of exciplexes is usually understood in terms of the redox potential, defined as the difference between the ionization potential of the donor and electron affinity of the acceptor[18]. For exciplexes in solutions, a unit-slope dependence of the exciplex emission on the redox potentials is observed. Moreover, recent work by Sreearunothai *et al.*[11] suggested that different orientations of the molecules at the heterojunction result in either repulsive or attractive interchain interactions. Their calculations of the Coulomb interaction between excitonic excited states on one chain and the ground state on the other revealed that whereas the former leads to a blue-shifted exciton emission the latter favours the formation of exciplex states, thereby enhancing the charge separation process.

Our models produce descriptions of the exciplex that match experiments very directly—including the 30° off-chain axis orientation of the dipole transition that we also report experimentally here. However, for the PFB:F8BT system they also reveal the occurrence of energetically similar but non-emissive charge-transfer states, the presence of which explains the long-standing puzzle of the low electroluminescence efficiency of this system[19]. Our evidence that there can be a range of coulombically bound both emissive and non-emissive charge-transfer states provides a general framework for the description of charge capture or separation at heterojunctions.

For the PFB:F8BT system, we first calculated the polarization energy induced by the presence of F8BT on the PFB exciton for varying relative displacements of the PFB chain in the xy plane parallel to the F8BT backbone. The cross-section along the main chain axis direction (x) of the Coulomb interaction for a lateral displacement $y = +1$ Å is shown in Fig. 2a. The results indicate

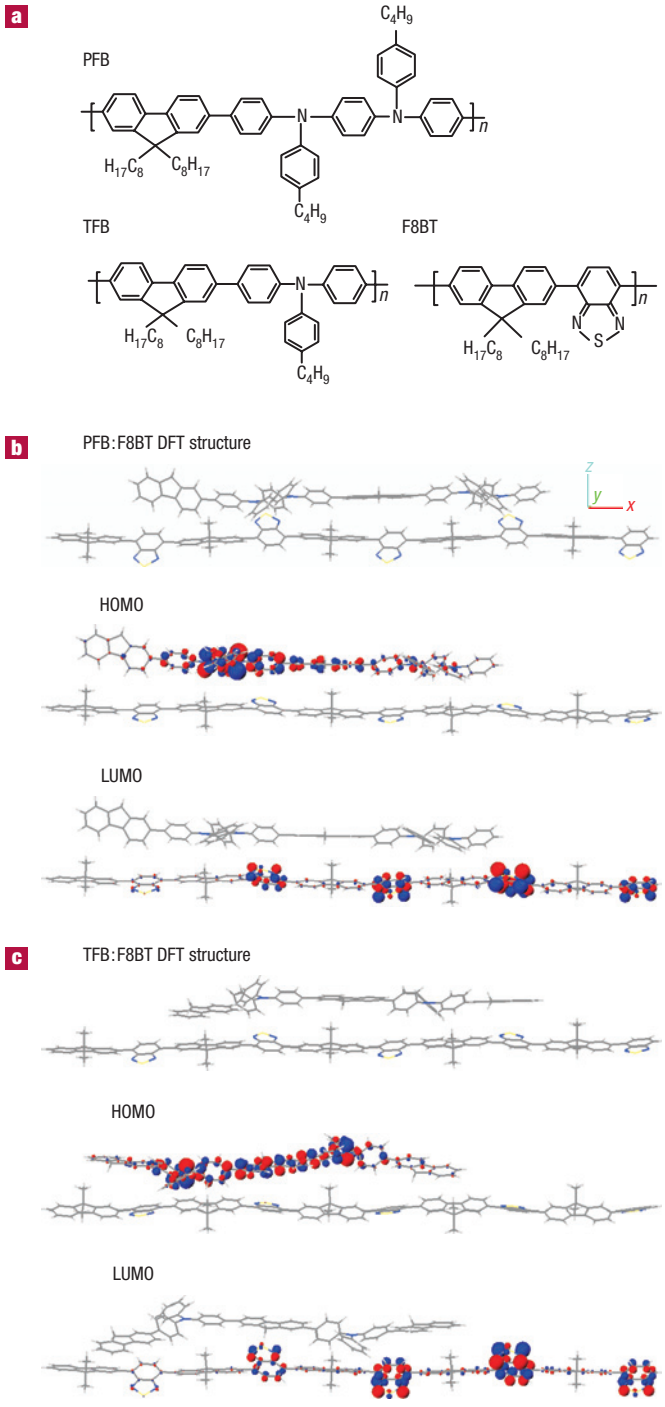

Figure 1 Chemical/density functional theory (DFT) structures of investigated systems and their HOMO/LUMO orbitals. a, Chemical structures of PFB, TFB and F8BT. The investigated system contains two and five repeat units of PFB/TFB and F8BT, respectively. **b**,**c**, Ground-state structures of blends obtained from DFT simulation and their corresponding HOMO and LUMO orbitals calculated at the intermediate neglect of differential overlap (INDO)/ single-configuration interaction (SCI) level of PFB:F8BT (**b**) and TFB:F8BT (**c**). The size and colour of the circles describe the amplitude and sign, respectively, of the linear combination of atomic orbitals coefficients associated with the π atomic orbitals.

that different orientations of the interacting chains give rise to either attractive or repulsive interactions, as reported previously[11]. The (permanent-) charge–(induced-) charge interaction causes a red-shift (by up to 90 meV) of the PFB electronic transition in the attractive configurations, whereas it results in a blue-shifted PFB optical transition (by up to 12 meV) in the repulsive configurations.

We now compare the charge redistribution on going from the ground state to the excited states in these two types of configuration in Fig. 3a,b. In the attractive configurations, we observe that the lowest excited state has a pronounced charge-transfer character with partial negative charges localized on one BT unit of F8BT in close interaction with the neighbouring positively charged triarylamine group of PFB. This state is primarily described by a single electronic configuration where one electron is excited from the PFB-localized HOMO to the F8BT-localized LUMO (Fig. 1b). We note that the second excited state of the attractive configurations corresponds to localized excitations on F8BT with small interchain charge-transfer character. For the repulsive configurations, the ordering of the lowest electronic excitations is reversed with respect to the attractive case, with the localized F8BT exciton lying at lower energy.

We have calculated characteristics of the lowest singlet excited states, that is, excitation energy, radiative lifetime and charge redistribution, as a function of a range of x, y displacements. Cross-sections along the main-chain-axis direction (x) of these properties for a lateral displacement $y = +1$ Å are shown in Fig. 2b–d and reveal three distinct regimes. In the first regime (I, $x \leq -5$ Å and $x \geq 6$ Å), the first electronic transition occurs at an energy of ~2.3 eV and has a radiative lifetime of the order of 1–2 ns. These electronic excitations form in the repulsive range identified above and have a dominant excitonic character (with radiative lifetimes comparable to the experimental values for bulk F8BT excitons[1]). In the second regime (II, -4 Å $\leq x \leq -2$ Å and 2 Å $\leq x \leq 5$ Å), the calculated lifetimes span a range from ~40 to a few hundred nanoseconds. We identify these excited states as the emissive exciplexes reported previously[1]. The radiative lifetime of these exciplex-like electronic states, at some 100 times longer than that of excitons, is in excellent agreement with the experimental data. Finally, for the configurations falling in regime III, the lowest excited state is characterized by an excitation energy similar to that of the exciplexes, yet has a much longer lifetime and smaller oscillator strength. We identify these species as 'polaron-pair' excited states[20]. This polaron-pair excitation can be regarded as a special case of the more general exciplex but where a complete charge transfer occurs from the donor to the acceptor. We note that the geometrical structures favouring electronic excitations in regime II and III both correspond to attractive configurations.

The electronic states of excited-state complexes with charge-transfer character are usually described by equation (1), which is essentially a linear combination of pure ion pairs and locally electronic configurations of the donor and acceptor (ignoring other configurations that do not contribute significantly).

$$|\mathrm{XP}\rangle = c_{\mathrm{CT}}|\mathrm{PFB} \rightarrow \mathrm{F8BT}\rangle + c_{\mathrm{EX}}|\mathrm{F8BT} \rightarrow \mathrm{F8BT}\rangle . \qquad (1)$$

The expansion coefficients c_{CT} and c_{EX} determine the relative weights of charge-transfer and local electronic excitations to the lowest eigenstate of the complex, $|\mathrm{XP}\rangle$. The polaron pair corresponds to $c_{\mathrm{CT}} \sim 1$; that is, full charge transfer occurs from the donor to the acceptor. In Fig. 2e, we report the INDO/SCI charge redistribution calculated on going from the ground state to the lowest excited state of representative geometries of the PFB:F8BT system. It can be seen that, whereas hardly any intermolecular rearrangement of the charge distribution takes place in excitonic states where repulsive configurations are favoured, a close to complete charge transfer occurs from PFB to F8BT in the attractive configurations stabilizing polaron-pair formation. In

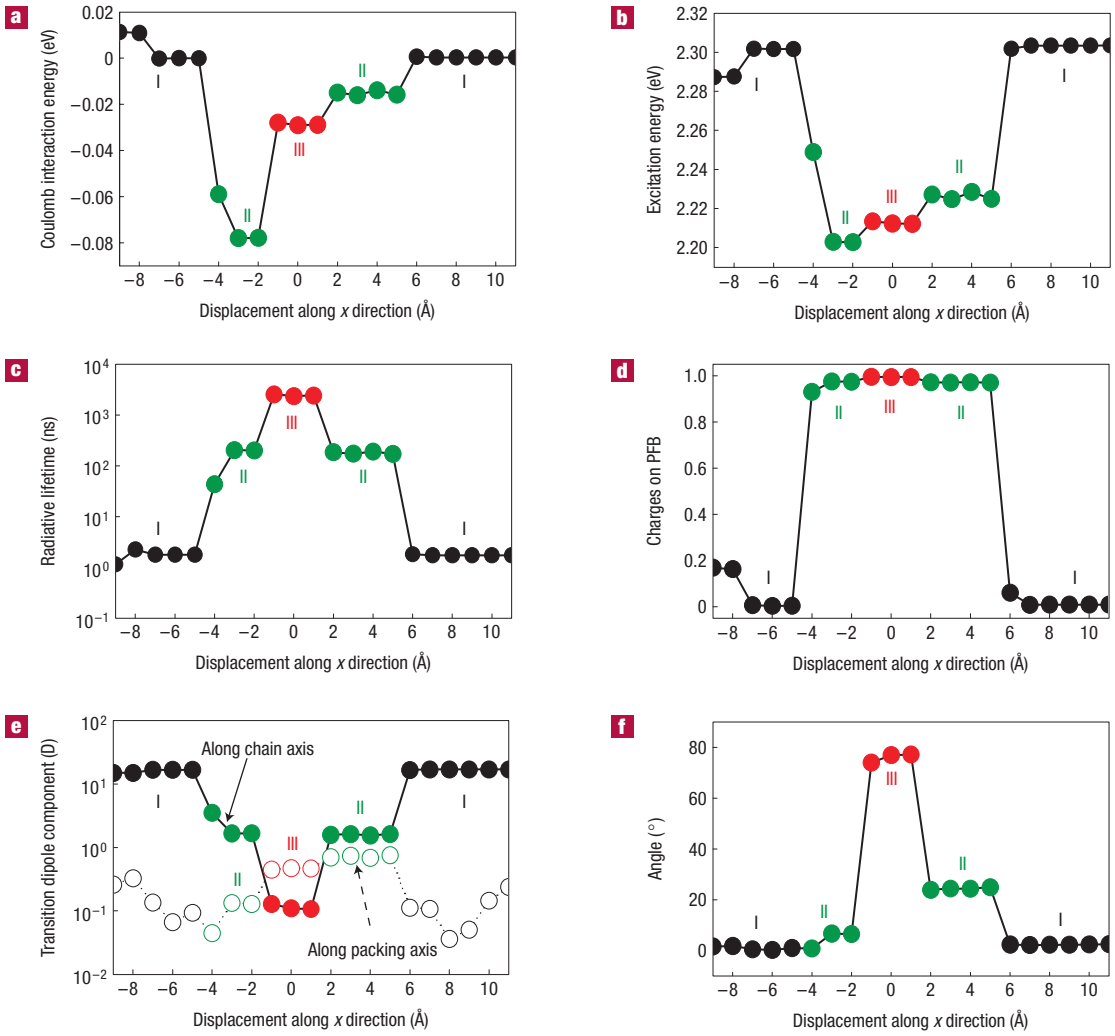

Figure 2 Coulomb interaction energy and excited-state properties of representative PFB:F8BT structures. a–d, Cross-sections of the Coulomb interaction energy, excitation energy, radiative lifetime and charge redistribution of PFB respectively in their lowest excited states as a function of the displacements with respect to the minimized original DFT/PCFF PFB:F8BT structure along $y = +1$ Å. **e**, Components of the INDO/SCI transition dipole moment along the chain axis (filled circles) and along the packing direction (open circles). **f**, Rotation angles between the transition dipole moment and the chain axis. There are three regimes: (I) black circles denote excitonic states; (II) green circles denote exciplex states; (III) red circles represent polaron-pair states.

the intermediate cases (regime II), exciplex states with dominant charge-transfer character yet with a small fraction of locally excited F8BT electronic excitation are found.

By expanding $|XP\rangle$ in a molecular orbital basis and assuming for simplicity a three-orbital model (that is, the charge-transfer $|PFB \rightarrow F8BT\rangle$ excitation corresponds to $|H_{PFB} \rightarrow L_{F8BT}\rangle$ and the localized $|F8BT \rightarrow F8BT\rangle$ excitation is $|H_{F8BT} \rightarrow L_{F8BT}\rangle$, where H_{PFB}, H_{F8BT} and L_{F8BT} denote the HOMOs of PFB and F8BT and the LUMO of F8BT, respectively), the overall transition dipole moment to the lowest excited state in the complex can be recast from first-order perturbation theory as

$$\langle S_0|\mu|XP\rangle = c_{CT}\langle H_{PFB}|\mu|L_{F8BT}\rangle + c_{EX}\langle H_{F8BT}|\mu|L_{F8BT}\rangle$$
$$\approx c_{CT}\langle H_{PFB}|\mu|L_{F8BT}\rangle + \frac{\langle H_{PFB}|t|H_{F8BT}\rangle}{E_{EX}-E_{CT}}\langle H_{F8BT}|\mu|L_{F8BT}\rangle, \quad (2)$$

where E_{EX} and E_{CT} denote the energies of pure local and charge-transfer electronic configurations, respectively, $\langle H_{F8BT}|\mu|L_{F8BT}\rangle$ is the transition dipole moment of F8BT, $\langle H_{PFB}|t|H_{F8BT}\rangle$ is the (one-electron) matrix element mixing the HOMOs of the PFB and F8BT chains and $c_{CT} \leq 1$. Therefore, the exciplex states acquire absorption cross-sections and finite radiative lifetimes through either direct overlap between the HOMO and LUMO of the interacting molecules (first term in equation (2)) or mixing with the F8BT localized excitation (second term in equation (2)). Note that admixture of PFB-localized excitations can be ruled out, as these occur at much higher energy.

It is interesting to consider the polarization of the two contributions in equation (2): whereas the direct overlap term contributes a transition dipole moment component along the packing axis (z axis here), the interaction between local and charge-transfer configurations provides an xy-polarized component resulting from intensity borrowing from the F8BT excitonic transition. In Fig. 2e, the INDO/SCI average values of the transition

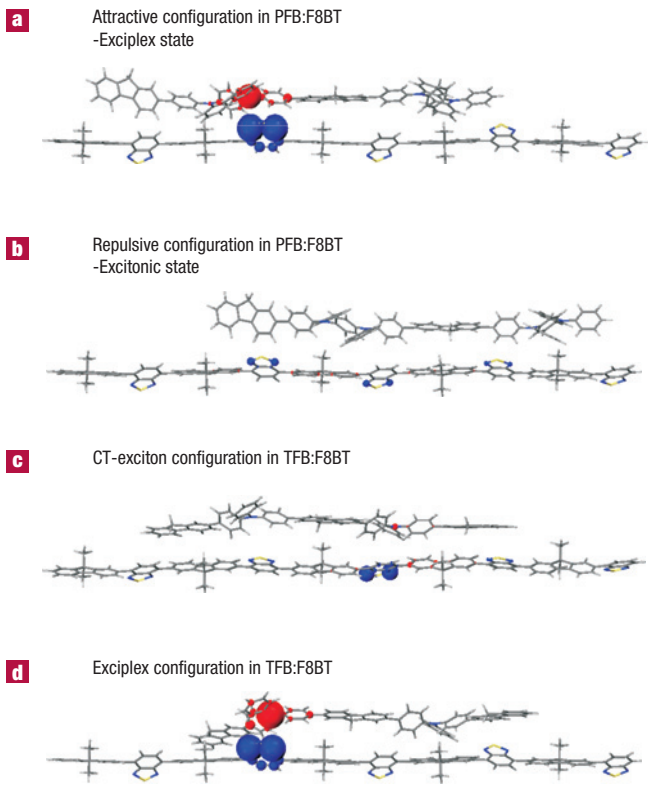

Figure 3 Charge redistributions of the lowest excited states of representative configurations. a–d, The charge differences between the ground and lowest excited states of representative attractive and repulsive configurations of PFB:F8BT blends, and those of CT-exciton and exciplex patterns of TFB:F8BT blends, respectively. Red and blue circles represent positive and negative charges, respectively.

dipole components along the stacking axis and in the perpendicular molecular planes are shown for representative configurations. It is seen that the transition dipole moment to the exciplex states arises primarily from the mixing between charge-transfer and excitonic configurations, that is, it is mostly polarized in the xy plane (the second term in equation (2) dominates). In contrast, pure polaron-pair configurations show transition dipole moments that are smaller and oriented along the packing axis, as they result from direct overlap between the HOMO orbital of PFB and the LUMO orbital of F8BT. The angle θ in between the transition dipole moment and the chain axis direction is smaller than 3° for the excitonic states, close to 75° for polaron-pair states and intermediate for exciplexes (Fig. 2f).

We are able to compare these values against experimental results for exciplex emission through measurements of luminescence depolarization. At times beyond a few nanoseconds, all emission in PFB:F8BT blends is due to exciplexes, which either emit directly in a band peaking near 645 nm or, if thermally excited, transfer as excitons to the F8BT and cause emission near 550 nm (ref. 9). Thus both 'regenerated' exciton and exciplex emission arise from the same excitation population, and differences in their depolarization behaviour enable us to determine the angle θ. Figure 4 shows the photoluminescence decays and their corresponding polarization anisotropy kinetics for the PFB:F8BT blends with two blend ratios. We present kinetics recorded at 645 and 550 nm to differentiate the exciplex from regenerated exciton photoluminescence. After an initial decay, which is determined by the instrument response, we record a constant value for the emission anisotropy in all cases. We conclude that the exciplex is, in contrast to excitons, immobile. This strongly supports our overall conclusion that the local electronic properties of the heterojunction states are crucial for the overall device performance (see below). The delayed photoluminescence in the blend containing 10% of F8BT is more polarized than that in the 50%:50% blend. This is because the domain size is smaller in the former, and excitons therefore retain more polarization information when migrating to the heterojunction. For both blend ratios, a higher anisotropy is observed for the emission of the regenerated excitons compared with the exciplex. Averaged over a time interval from 2 to 45 ns, the blend containing 10% F8BT gives anisotropy values of 0.23 and 0.06 for the exciton and exciplex emission, respectively. For the blend with 50% F8BT, the corresponding values are 0.06 and 0.02. The lower anisotropy values for the exciplex emission with respect to the exciton emission are a direct indication of a significant off-chain component in the transition dipole moment of the exciplex. θ can be calculated from the experimental data as $\theta = \cos^{-1}(\pm\sqrt{(r_E + 2r_X)/3r_E})$, where r_E and r_X are the polarization anisotropy values for exciton and exciplex photoluminescence, respectively[21]. We obtain $\theta = 45°$ and 44° for the blend containing 10% and 50% F8BT, respectively. This directly shows that the exciplex state has a significant transition dipole moment perpendicular to the excitonic (in-chain) direction, and confirms our theoretical calculations.

It has been shown that pure polaron-pair excited states in molecular systems showing charge-transfer character excitations have charge-transfer character in excess of 90% (ref. 20). The results reported here in our polymer system show that, in the attractive basin, the wavefunction of the lowest singlet excitation shows in all cases a charge-transfer component ranging from 95 to 100% and that subtle changes in the relative orientations of the polymer chains are enough to tune the excited-state lifetime over at least one order of magnitude. Namely, the radiative lifetime of the lowest electronic transition is found to be ~10 times longer when the relative displacement of the PFB chain with respect to the F8BT chain switches from $x = \pm 2$ Å (exciplex state) to $x = 0$ Å (polaron-pair state). As these excited species with variable charge-transfer character have similar energies, well below that of the F8BT excitons, they should act as singlet excitation reservoirs[9] with (radiative) lifetimes spanning from a few tens to a few thousands of nanoseconds. Note that the stabilization energy of the exciplex with respect to the exciton is estimated to be 100 meV from our quantum-chemical simulations, whereas experimentally it is 250 ± 30 meV (ref. 1). The underestimated stabilization energy might be due to the fact that the calculations were carried out on the ground-state geometries; see the Methods section.

We now move to the case of the TFB:F8BT blend. We have calculated the polarization energy induced by the presence of F8BT on the TFB exciton as well as the characteristics of the lowest singlet excited state as a function of a range of x, y displacements. Cross-sections along the main-chain-axis direction (x) of these properties for a lateral displacement $y = -3$ Å are shown in Fig. 5a–d. Again, three distinct species can be identified from these figures. For the first species (I, $x \leq -4$ Å, -2 Å $\leq x \leq -1$ Å, $x = 2$ Å and $x \geq 5$ Å), the first electronic transition occurs at an energy of ~2.46 eV and shows a radiative lifetime at around 1.5 ns. The electronic excitations formed in this regime feature a dominant excitonic character. For the second species (II, 0 Å $\leq x \leq 1$ Å), the calculated lifetimes are a few hundred nanoseconds; as in the PFB:F8BT case, we identify the corresponding excited-state species as the emissive exciplexes[1] (the calculated lifetime of exciplex configurations for the whole xy plane in fact spans from 36 to a few hundred nanoseconds). The stabilization energy of exciplexes in the TFB:F8BT blend is about 50 meV, which is underestimated

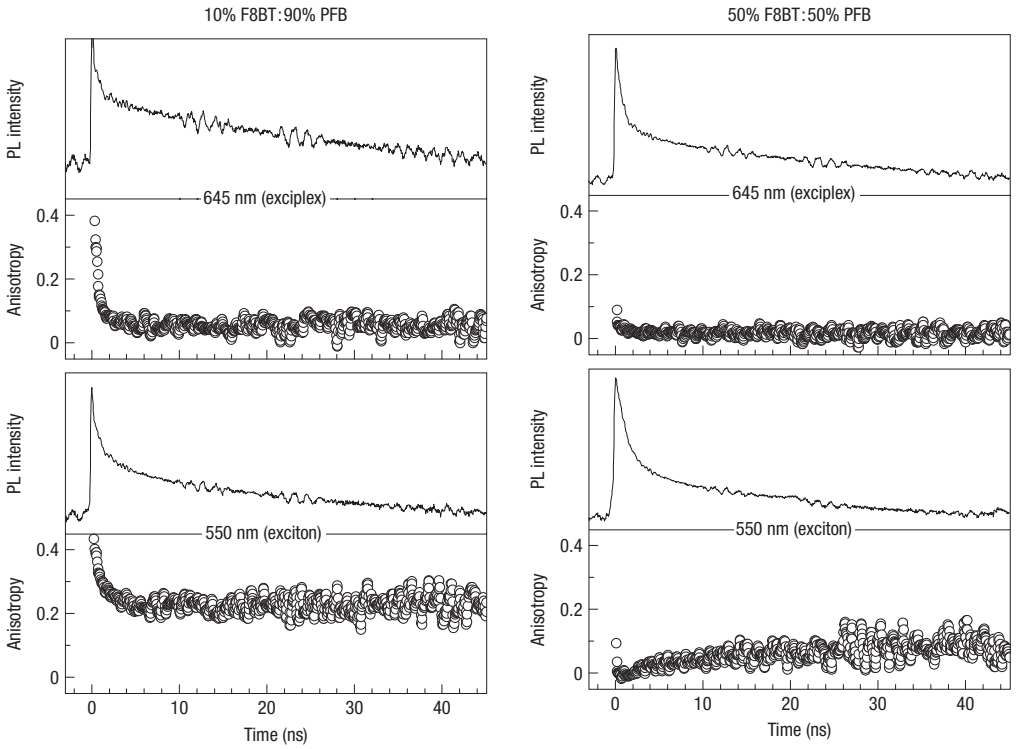

Figure 4 Polarization-resolved time-resolved photoluminescence of interface states. The magic angle and polarization anisotropy decay of the photoluminescence are shown as a function of time for the two blend ratios and wavelengths as indicated in the figure. Time-resolved PL anisotropy decay is defined by $(I_{par} - I_{perp})/(I_{par} + 2I_{perp})$, where $I_{par(perp)}$ is the PL intensity recorded with the laser polarization parallel (orthogonal) to that of the detection analyser[30]. The excitation wavelength for these kinetic measurements was 470 nm to ensure site-selective excitation of the low-band-gap polymer F8BT, whose absorption peaks at 480 nm.

compared with experimental data, 100 ± 20 meV (ref. 1). For the fourth species that we find in the blends studied in this report (IV, $x = -3$ Å and 3 Å $\leq x \leq 4$ Å) the lowest excited state, which we refer to as the CT-exciton state in the following, cannot strictly be classified as either an exciton or an exciplex state, as its wavefunction comprises large contributions from both localized and charge-transfer excitations, as is illustrated in Fig. 3c. Unlike exciplexes, which have a dominant interchain charge-transfer character with very little intrachain excitonic character (Fig. 3d), the CT-exciton state identified in regime IV of Fig. 5b–d shows a much more modest amount of intermolecular charge transfer. This species has a radiative lifetime of the order of 2–3.5 ns and an oscillator strength ~1.5 times lower than that of the pure singlet excitons. In Fig. 5e, the INDO/SCI average values of the transition dipole components along the stacking axis and in perpendicular molecular planes are plotted for representative configurations. The transition dipole moment to the CT-exciton state arises mainly from the mixing between charge-transfer and excitonic configurations and is much more polarized in the xy plane than that of the exciplex. We note that this CT-exciton state has not been identified in TFB:F8BT blends, probably because the photoluminescence spectra of the blend and F8BT excitons strongly overlap, thus making it difficult to disentangle the two contributions. We also looked for the presence of polaron pairs; however, this species is rarely observed in TFB:F8BT blends according to our calculations, as discussed below.

The nature of the lowest electronic excitations in the PFB:F8BT and TFB:F8BT systems is summarized in Fig. 6. We have examined 231 geometries for the PFB:F8BT system, of which 36 geometries are categorized as polaron pairs and 51 correspond to exciplexes. On the other hand, from the 546 geometries considered in the TFB:F8BT case, only two geometries are long-lived polaron pairs, 54 are identified as exciplexes and 51 are categorized as CT-exciton states. As sketched in Fig. 6, the main difference between the two types of blend is the presence in PFB:F8BT of fully charge-transfer excited states and the absence of the mixed-type excited species that are intermediate between excitons and exciplexes. In other words, the lowest electronic excited state in the PFB:F8BT blends reveals in most cases a smaller admixture from F8BT localized excitations into charge-transfer excitations. This can be traced back to the greater redox potential for the PFB:F8BT pair compared with TFB:F8BT, hence a greater energy mismatch between local and charge-transfer excitations at the denominator of the second term in equation (1).

It has been shown[1,9] that light-emitting diodes made with TFB:F8BT blends can show high electroluminescence efficiency, above $19\,\mathrm{lm\,W^{-1}}$, and that the electroluminescence is due to emission from exciplexes and regenerated excitons at the heterojunction. This high electroluminescence efficiency is consistent with the presence of only emissive states at the heterojunction. In contrast, PFB:F8BT light-emitting diodes show an electroluminescence efficiency an order of magnitude lower[1,9]. We attribute this to the presence of the non-radiative polaron pairs in PFB:F8BT blends, because this non-radiative decay channel will diminish the electroluminescence efficiency. Similar reductions in photoluminescence efficiencies are seen for PFB:F8BT blends, from up to 80% for F8BT to a few per cent for blends, and this has previously been considered to be an indication of high charge-separation yield in the PFB:F8BT blends. However, the photovoltaic performance of diodes made with either blend is

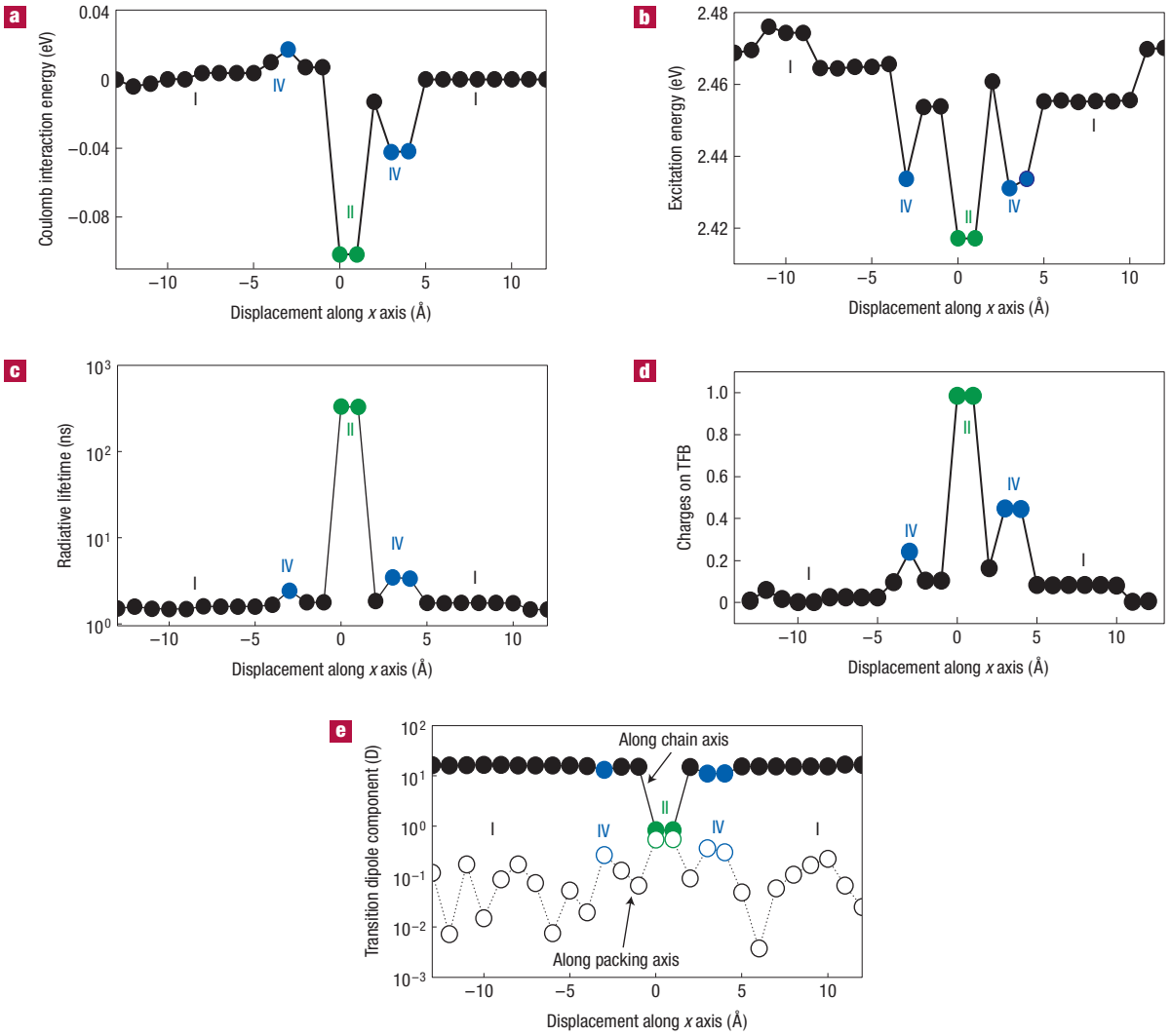

Figure 5 Coulomb interaction energy and excited-state properties of representative TFB:F8BT structures. a–d, Cross-sections of the Coulomb interaction energy, excitation energy, radiative lifetime and charge redistribution of the TFB in the lowest excited states as a function of the displacements with respect to the minimized original DFT/PCFF TFB:F8BT structure along $y = -3$ Å. **e**, Components of the INDO/SCI transition dipole moment along the chain axis (filled circles) and along the packing direction (open circles). There are three regimes: (I) black circles denote excitonic states; (II) green circles denote exciplex states; (IV) blue circles represent the CT-exciton state.

relatively poor, with an external quantum efficiency (charges collected per incident photon) no higher than 10% under short-circuit conditions[19]. We note that exciplex states are strongly bound at room temperature, as observed from electric-field-dependent luminescence-decay measurements[9], and once formed are unlikely to contribute to the collected photocurrent. We consider that the binding energy (with respect to a well-separated charge pair) is due to the strong coulombic attraction between an electron and a hole on adjacent chains across the heterojunction. We expect a very similar coulombic binding energy for the polaron pairs, because the spatial distribution of their electron and hole wavefunction is very similar. This is consistent with the low photovoltaic efficiencies seen for both systems. More generally, bound electron–hole pairs are considered to reduce photovoltaic efficiency in heterojunction diodes[22]. Our model has provided the first microscopic description of the nature of excitonic states at molecular semiconductor heterojunction states, and reveals that there is a range of excitonic states possible, as determined by specific features of intermolecular overlap.

METHODS

THEORETICAL CALCULATIONS

The structures investigated in this report comprise two polymer chains: a PFB/TFB molecule with two repeating units and an F8BT molecule with five repeating units (because of the limited delocalization of the π system, these oligomers are very reasonable models for the corresponding polymers). The simulations were carried out by first optimizing the ground-state geometry of the isolated PFB/TFB and F8BT chains at the B3LYP (6-31G basis set) DFT level[23,24]. The resulting geometries are shown at the top of Fig. 1b,c. As the alkyl side chains do not contribute significantly to the electronic excitation, they were excluded for both molecules from our calculations to reduce computation efforts[25]. We examined the influence of the relative orientations of two interacting molecules by translating the PFB/TFB molecule in the (xy) plane parallel to the F8BT backbone. The potential energy surface for such xy displacements was explored using a polymer-consistent force-field (PCFF)[26] molecular-mechanics approach on the basis of a 9–6 Lennard-Jones potential for van der Waals contributions and electrostatic interactions between atomic charges. These structures were relaxed while maintaining the backbones of the two molecules frozen at their DFT values (therefore only the intermolecular structural arrangements, namely the interchain distances

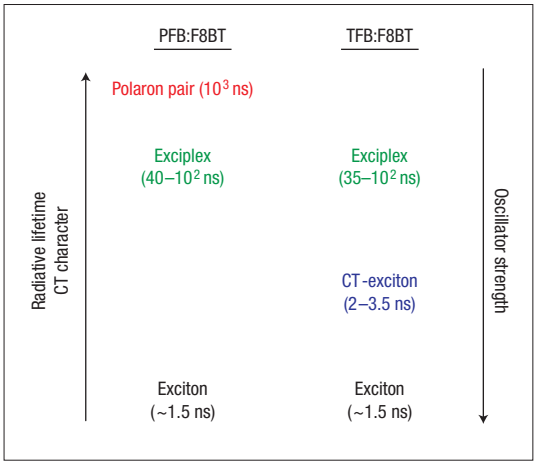

Figure 6 Schematic diagram of the lowest electronic excitations in the PFB:F8BT and TFB:F8BT systems. The diagram describes the properties of the four electronic excitations taking place at the heterojunctions of PFB:F8BT and TFB:F8BT blends.

and relative orientations of the two molecular cores, were optimized). After geometry optimization, the distance between the PFB/TFB and F8BT backbones was found to be in the range of 4.4–5 Å. Note that this is a very crude model, as we ignored both on-chain and interchain geometric relaxation phenomena taking place following photoexcitation of the physical dimer. Although this might impact the energetics somewhat, it should not drastically affect the overall picture. The coulombic 'solvation' energy associated with the interaction between the (permanent) ground-state charge distribution of one chain and the (transient) charge redistribution on photoexcitation of the other (interacting) chain was calculated as described in ref. 11. This provides the spectral shift on the localized PFB/TFB (F8BT) exciton emission as induced by solvation with F8BT (PFB/TFB), which is positive (that is, blue-shift) for repulsive and negative (red-shift) for attractive configurations. For the attractive configurations, the triarylamine groups of PFB/TFB are found to be in proximity with the neighbouring BT units of the F8BT chain. On the other hand, the F8 units of PFB/TFB lie on top of the BT units of F8BT in the repulsive configurations.

On the basis of the ground-state minimized geometries, a semiempirical INDO hamiltonian[27] (with a screened Mataga–Nishmoto potential to describe electron–electron interactions in organic condensed phase)[11,28,29] was combined with an SCI scheme to characterize the excited-state properties of the two-chain systems, including charge distributions, excitation energies and transition dipole moments. As demonstrated in Fig. 1b,c, the LUMO is localized on the BT units of the F8BT chain whereas the HOMO is delocalized on the PFB and TFB chain, with large weights on the triarylamine groups. Thus, we expect that the nature of the lowest electronic excitations, and more specifically the admixture between charge-transfer and localized configurations, will be sensitive to the relative orientations and distances between the benzothiadiazole units of F8BT and the triarylamine units of PFB and TFB. The computed excitation energies and transition dipole moments were then injected into Einstein coefficients for the calculation of the radiative lifetimes. The interchain distance dependence has also been examined for the excited-state properties of the electronic excitations that form at the heterojunction. If the interchain distance was decreased by 0.01 nm, for the exciplex excitation, the sensitivity of the interchain separation to the radiative lifetime was found to be of the order of 10%, intermediate between polaron pairs, whose radiative lifetime decreased by ~35%, and excitons, whose radiative lifetime stayed nearly constant.

PHOTOLUMINESCENCE DECAYS AND POLARIZATION ANISOTROPY KINETICS

Time-resolved photoluminescence-decay and corresponding polarization-anisotropy-kinetics measurements[30] were carried out using a time-correlated single-photon-counting set-up described elsewhere[31].

Received 25 June 2007; accepted 20 March 2008; published 27 April 2008.

References

1. Morteani, A. C. *et al.* Barrier-free electron–hole capture in polymer blend heterojunction light-emitting diodes. *Adv. Mater.* **15**, 1708–1712 (2003).
2. Halls, J. J. M. *et al.* Efficient photodiodes from interpenetrating polymer networks. *Nature* **376**, 498–500 (1995).
3. Arias, A. C. *et al.* Photovoltaic performance and morphology of polyfluorene blends: A combined microscopic and photovoltaic investigation. *Macromolecules* **34**, 6005–6013 (2001).
4. Brabec, C. J., Sariciftci, N. S. & Hummelen, J. C. Plastic solar cells. *Adv. Funct. Mater.* **11**, 15–26 (2001).
5. Halls, J. J. M. *et al.* Charge- and energy-transfer processes at polymer/polymer interfaces: A joint experimental and theoretical study. *Phys. Rev. B* **60**, 5721–5727 (1999).
6. Cao, Y., Parker, I. D., Yu, G., Zhang, C. & Heeger, A. J. Improved quantum efficiency for electroluminescence in semiconducting polymers. *Nature* **397**, 414–417 (1999).
7. Palilis, L. C. *et al.* High performance blue light-emitting diodes based on conjugated polymer blends. *Synth. Met.* **121**, 1729–1730 (2001).
8. McNeill, C. R., Westenhoff, S., Groves, C., Friend, R. H. & Greenham, N. C. Influence of nanoscale phase separation on the charge generation dynamics and photovoltaic performance of conjugated polymer blends: Balancing charge generation and separation. *J. Phys. Chem. C* **111**, 19153–19160 (2007).
9. Morteani, A. C., Sreearunothai, P., Herz, L. M., Friend, R. H. & Silva, C. Exciton regeneration at polymeric semiconductor heterojunctions. *Phys. Rev. Lett.* **92**, 247402 (2004).
10. Morteani, A. C., Friend, R. H. & Silva, C. Endothermic exciplex–exciton energy-transfer in a blue-emitting polymeric heterojunction system. *Chem. Phys. Lett.* **391**, 81–84 (2004).
11. Sreearunothai, P. *et al.* Influence of copolymer interface orientation on the optical emission of polymeric semiconductor heterojunctions. *Phys. Rev. Lett.* **96**, 117403 (2006).
12. Bittner, E. R., Ramon, J. G. S. & Karabunarliev, S. Exciton dissociation dynamics in model donor–acceptor polymer heterojunctions. I. Energetics and spectra. *J. Chem. Phys.* **122**, 214719 (2005).
13. Ramon, J. G. S. & Bittner, E. R. Excited state calculations on fluorene-based polymer blends: Effect of stacking orientation and solvation. *J. Chem. Phys.* **126**, 181101 (2007).
14. Jenekhe, S. A. & Osaheni, J. A. Excimers and exciplexes of conjugated polymers. *Science* **265**, 765–768 (1994).
15. Granlund, T., Pettersson, L. A. A., Anderson, M. R. & Inganäs, O. Interference phenomenon determines the color in an organic light emitting diode. *J. Appl. Phys.* **81**, 8097–8104 (1997).
16. Gebler, D. D., Wang, Y. Z., Fu, D.-K., Swager, T. M. & Epstein, A. J. Exciplex emission from bilayers of poly(vinyl carbazole) and pyridine based conjugated copolymers. *J. Chem. Phys.* **108**, 7842–7848 (1998).
17. Offermans, T., van Hal, P. A., Meskers, S. C. J., Koetse, M. M. & Janssen, R. A. J. Exciplex dynamics in a blend of π-conjugated polymers with electron donating and accepting properties: MDMO-PPV and PCNEPV. *Phys. Rev. B* **72**, 045213 (2005).
18. Weller, A. *The Exciplex* 23–38 (Academic, New York, 1975).
19. Xia, Y. & Friend, R. H. Controlled phase separation of polyfluorene blends via inkjet printing. *Macromolecules* **38**, 6466–6471 (2005).
20. Gould, I. R., Young, R. H., Mueller, L. J., Albrecht, A. C. & Farid, S. Electronic structure of exciplexes and excited charge-transfer complexes. *J. Am. Chem. Soc.* **116**, 8188–8199 (1994).
21. Valeur, B. *Molecular Fluorescence* Ch. 5 (Wiley-VCH Verlag GmbH, Weinheim, 2002).
22. Mihailetchi, V. D., Koster, L. J. A., Hummelen, J. C. & Blom, P. W. M. Photocurrent generation in polymer–fullerene bulk heterojunctions. *Phys. Rev. Lett.* **93**, 216601 (2004).
23. Becke, A. D. Density-functional thermochemistry. III. The role of exact exchange. *J. Chem. Phys.* **98**, 5648–5652 (1993).
24. Lee, C., Yang, W. & Parr, R. G. Development of the Colle–Salvetti correlation-energy formula into a functional of the electron density. *Phys. Rev. B* **37**, 785–789 (1988).
25. Cornil, J. *et al.* Electronic and optical properties of polyfluorene and fluorene-based copolymers: A quantum-chemical characterization. *J. Chem. Phys.* **118**, 6615–6623 (2003).
26. Accelrys, Inc. *Cerius2 and Discover (programs) and Discover User Guide* (Molecular Simulations, Inc., San Diego, 1996).
27. Ridley, J. & Zerner, M. C. An intermediate neglect of differential overlap technique for spectroscopy: Pyrrole and the azines. *Theor. Chim. Acta* **32**, 111–134 (1973).
28. Mataga, N. & Nishimoto, K. Electronic structure and spectra of nitrogen heterocycles. *Z. Phys. Chem. Neue. Folge.* **13**, 140–157 (1957).
29. Chandross, M. & Mazumdar, S. Coulomb interactions and linear, nonlinear, and triplet absorption in poly(para-phenylenevinylene). *Phys. Rev. B* **55**, 1497–1504 (1997).
30. Westenhoff, S. *et al.* Supramolecular electronic coupling in chiral oligothiophene nanostructures. *Adv. Mater.* **18**, 1281–1285 (2006).
31. Silva, C. *et al.* Exciton and polaron dynamics in a step-ladder polymeric semiconductor: The influence of interchain order. *J. Phys. Condens. Matter* **14**, 9803–9824 (2002).

Acknowledgements

We thank J. S. Kim and W. J. D. Beenken for discussions. This work was supported by the Engineering and Physical Science Research Council, and by the EU Integrated Project NAIMO (No NMP4-CT-2004-500355). The work in Mons was partly supported by the Belgian Federal Government 'Interuniversity Attraction Pole in Supramolecular Chemistry and Catalysis, PAI 5/3', the Belgian National Fund for Scientific Research (FNRS/FRFC) and the European STREP project MODECOM (NMP-CT-2006-016434). D.B. is a research director of FNRS.

Author contributions

Y.-S.H., I.A., P.S. and C.D. carried out the modelling. S.W. and J.M.H. measured the photoluminescence anisotropy. Y.-S.H., S.W., R.H.F. and D.B. analysed data, interpreted results and wrote the paper. All authors provided comments on the manuscript. R.H.F. contributed to the interpretation of the combined modelling and experimental work. D.B. and R.H.F. directed the research.

Author information

Reprints and permission information is available online at http://npg.nature.com/reprintsandpermissions. Correspondence and requests for materials should be addressed to R.H.F. or D.B.